Acoustic properties of saturated porous media

I. Malinouskaya[a,b], Li Xiang-Yu[a], V.V. Mourzenko[b], J.-F. Thovert[b], P.M. Adler[a]

a. *Institut P', Département Fluides, Thermique, Combustion, Branche Combustion, ENSMA - 1, av. Clément Ader - BP 40109, 86961 Futuroscope Cedex*
b. *UPMC Sisyphe, BP 105, 4 Place Jussieu, 75252 Paris Cedex 05*

Résumé :

Ce travail concerne la propagation des ondes acoustiques dans des milieux poreux. Les développements théoriques de travaux précédents sont généralisés pour établir des équations dynamiques poro-élastiques pour un fluide compressible dans l'espace éventuellement constitué de pores multiples indépendants, fermés ou percolants. Ces équations impliquent plusieurs coefficients effectifs à déterminer en résolvant des problèmes de fermeture à l'échelle microscopique. Des applications systématiques sont présentées pour des milieux reconstruits et réels.

Abstract :

This work addresses the propagation of acoustic waves in porous media. The theoretical developments of earlier works are generalized to establish dynamic poro-elastic equations for a compressible fluid in a pore space which may consist in multiple independent pore components, closed or percolating. These equations involve several effective coefficients, to be determined by solving closure problems on the microscale. Systematic applications are presented, for various kinds of model reconstructed media, and for real media imaged by microtomography.

Mots clefs : Porous medium, acoustics, poro-elasticity

1 Introduction

This work addresses the propagation of acoustic waves in saturated porous media, along the same lines as the earlier works [1, 2], with two significant extensions : the influence of the interstitial fluid compressibility is taken into account, and the pore space is not supposed to be totally connected. Instead, it may consist in multiple independent pore components, closed or percolating.

The first step is to derive the generalized dynamic poro-elastic equations, which describe on the Darcy scale the coupled medium deformations and fluid displacements under stress. On the microscopic scale, the governing equations are Navier's elastodynamic equation in the solid, which is considered as isotropic and linearly elastic, and Navier-Stokes equations in the interstitial Newtonian fluid. These equations are coupled by displacement and stress continuity conditions at the fluid/solid interface.

2 Acoustic properties of saturated media

The upscaling to Darcy scale is conducted in the framework of homogenization theory, and follows the methodology of [3]. The typical scale l of the microstructure is supposed to be much smaller than the wave length λ. In addition, the medium is supposed to be macroscopically uniform, and therefore it can be regarded as spatially periodic in the theoretical developments and in the numerical determination of the effective coefficients. Hence, a two-scale expansion can be used for all the quantities such as the stresses or displacements, in terms of a slow and a fast varying space variables $\mathbf{x}$ and $\mathbf{y}$ associated with the length scales λ and l, respectively. For instance, for an harmonic deformation with pulsation

ω, the displacement field $\mathbf{u}$ is a power series of the small parameter $\eta = l/2\pi\lambda$,

$$\mathbf{u}(\mathbf{x}, \mathbf{y}) = \sum_{j=0}^{\infty} \eta^j \mathbf{u}^{(j)}(\mathbf{x}, \mathbf{y}) e^{i\omega t} \tag{1}$$

where $\mathbf{u}^{(j)}$'s are $\mathbf{y}$-periodic. This development gives rise to a series of problems at successive orders in η. Their solution yields the effective coefficients involved in the macroscopic equations, which are obtained by a spatial averaging of the local problems. The dynamic, Darcy-scale poro-elastic equations are obtained eventually in the following form.

$$\boldsymbol{\nabla} \cdot \mathbf{D} : \mathbf{E}(\mathbf{U}) + \Sigma_{i=1}^N \boldsymbol{\nabla} \cdot \boldsymbol{\alpha}^i P^i = -\langle\rho\rangle\omega^2\mathbf{U} - \rho_f\omega^2\Sigma_{i=1}^N \mathbf{W^i}$$

$$i\omega\mathbf{W}^i = -\frac{1}{\mu_f}\mathbf{K}^i \cdot \left(\boldsymbol{\nabla}P^i - \rho_f\omega^2\mathbf{U}\right) \quad \text{(for } i = 1, \dots, N) \tag{2}$$

$$\boldsymbol{\nabla} \cdot \mathbf{W}^i = \mathbf{A}^i : \mathbf{E}(\mathbf{U}) + \Sigma_{j=1}^N B^{ij}P^j - \epsilon^i c_f P^i \quad \text{(for } i = 1, \dots, N)$$

where the index i refers to the pore component. P is the fluid pressure, $\mathbf{W}$ the fluid displacement relative to the solid, $\mathbf{K}$ the permeability tensor, $\mathbf{U}$ the solid displacement, ϵ the pore volume fraction, μ_f the fluid viscosity and c_f its compressibility.

These equations involve several effective coefficients, to be determined by solving closure problems on the microscale. $\mathbf{D}$ is the effective elastic tensor of the dry porous medium. It can be calculated by solving the elastostatic equations in the solid space, when prescribed macroscopic strain tensors $\mathbf{E}(\mathbf{U})$ are imposed. $\mathbf{A}^i : \mathbf{E}(\mathbf{U})$ is the change of the pore volume i induced by the global deformation $\mathbf{E}(\mathbf{U})$, within a change of sign, and can be readily obtained when computing $\mathbf{D}$. Six problems with shear and compressional loads should be solved in order to determine all the components of $\mathbf{D}$ and $\mathbf{A}$ (Figure 1a-b)
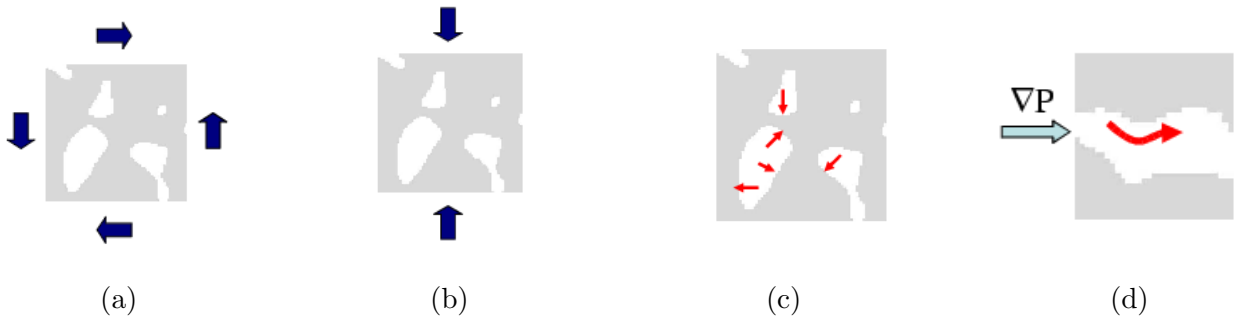

| (a) | (b) | (c) | (d) |

FIG. 1 – Porous media submitted to a shear (a) and a compressional (b) loads used to determine the complete tensor of elastic properties $\mathbf{D}$. (c) Porous medium submitted to interstitial pressure to obtain interaction coefficient B^{ij} and tensor $\boldsymbol{\alpha}$. (d) The flow under imposed pressure gradient to determine the permeability $\mathbf{K}$.

The tensor $\boldsymbol{\alpha}^i$ is the mean stress induced by a unit pressure imposed in pore i and the interaction coefficient B^{ij} is the change of the pore volume j induced by a unit pressure in pore i, within a change of sign (Figure 1c). Their determination requires the solution of an elastostatic problem, with zero mean strain and a unit pressure imposed successively in each of the N pore components.

Finally, $\mathbf{K}^i$ is the permeability tensor of the pore component i, complex and frequency dependent, to be determined by solving the flow equations for three prescribed pressure gradient directions, in each pore component and for each frequency under consideration (Figure 1d).

The last closure problem is the most demanding numerically. Fortunately, in most practical situations, there is at most one percolating pore component with a permeability to be determined (Figure 2). The other $\mathbf{K}^i$ are zero.
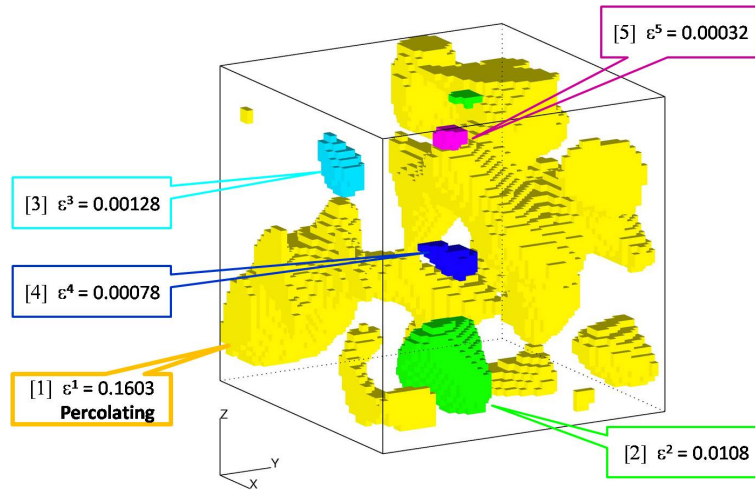
[5] ε⁵ = 0.00032

[3] ε³ = 0.00128

[4] ε⁴ = 0.00078

[1] ε¹ = 0.1603
Percolating

[2] ε² = 0.0108

FIG. 2 – Example of the media with 5 pore components where only one is percolating.

The elastic coefficients $\mathbf{D}$, $\boldsymbol{\alpha}^i$, $\mathbf{A}^i$ and B^{ij} have many properties and mutual relationships. Some of them are theoretical results, others are empirical observations. They can be used to reduce the number of closure problems to be solved, which can be very desirable in the case of many closed pores.

The first and most important property is

$$\boldsymbol{\alpha}^i = \mathbf{A}^i \tag{3}$$

This is a general result, which can be shown by using the Maxwell-Beti reciprocal theorem. Since $\boldsymbol{\alpha}^i$ is a stress tensor, $\boldsymbol{\alpha}^i$ and $\mathbf{A}^i$ are symmetric, as well as the matrix $\overline{\overline{B}}$

$$B^{ij} = B^{ji} \tag{4}$$

which is negative and diagonally dominant. These properties, their consequences and different approaches at various levels of approximation are described in a fully worked out example.

3 Simplifications and Applications

In the case of plane harmonic waves propagating along a direction $\mathbf{p}$, the solid and fluid displacements are of the form

$$\mathbf{u} = \mathbf{U}e^{i\omega t} = \hat{\mathbf{U}}e^{i(\omega t - k\mathbf{x}.\mathbf{p})} \tag{5}$$

$$\mathbf{w} = \mathbf{W}e^{i\omega t} = \hat{\mathbf{W}}e^{i(\omega t - k\mathbf{x}.\mathbf{p})} \tag{6}$$

The wave characteristics can be obtained by solving an eigenvalue problem corresponding to the Christoffel equation in the most general form

$$\begin{pmatrix} \mathbf{p}.\mathbf{D}^u.\mathbf{p}. & \mathbf{p}.\left(\Sigma_{i=1}^N \boldsymbol{\alpha}^i G^{1i}\right).\mathbf{p}. \\ -\frac{1}{\mu_f}\mathbf{p}.\mathbf{K}^1\left(\Sigma_{i=1}^N G^{1i}\mathbf{A}^i\right).\mathbf{p}. & \frac{1}{\mu_f}\mathbf{p}.\mathbf{K}^1 G^{11}\mathbf{p}. \end{pmatrix} \begin{pmatrix} \hat{\mathbf{U}} \\ \hat{\mathbf{W}}^1 \end{pmatrix} = c^2 \begin{pmatrix} \langle\rho\rangle & \rho_f \\ -\frac{\rho_f}{\mu_f}\mathbf{K}^1. & \frac{i}{\omega} \end{pmatrix} \begin{pmatrix} \hat{\mathbf{U}} \\ \hat{\mathbf{W}}^1 \end{pmatrix} \tag{7}$$

where $G^{ji} = \left(B^{ji} - c_f\delta^{ij}\epsilon^i\right)^{-1}$ and $\mathbf{D}^u = \mathbf{D} - \Sigma_i\Sigma_j\boldsymbol{\alpha}^i G^{ij}\mathbf{A}^j$.

The usual compression and shear waves can be observed, as well as the slow compression wave predicted by [4]. In anisotropic media, when the principal directions of the various tensors $\mathbf{D}$, $\boldsymbol{\alpha}^i$ and $\mathbf{K}^i$ are not aligned, the eigenmodes are always mixed waves. However, they are generally very close to one of the aforementioned simple waves.

Figure 3 is an example of compression and shear wave velocities, calculated from a sandstone sample which had been imaged by X-ray microtomography, in the low and intermediate frequency range where

they do not depend on ω. These general charts give the velocities as functions of the interstitial fluid density and compressibility. The positions of several real fluids of interest are marked, as well as that of water regarded as incompressible. Note that the shear wave velocity does not depend on the fluid compressibility.
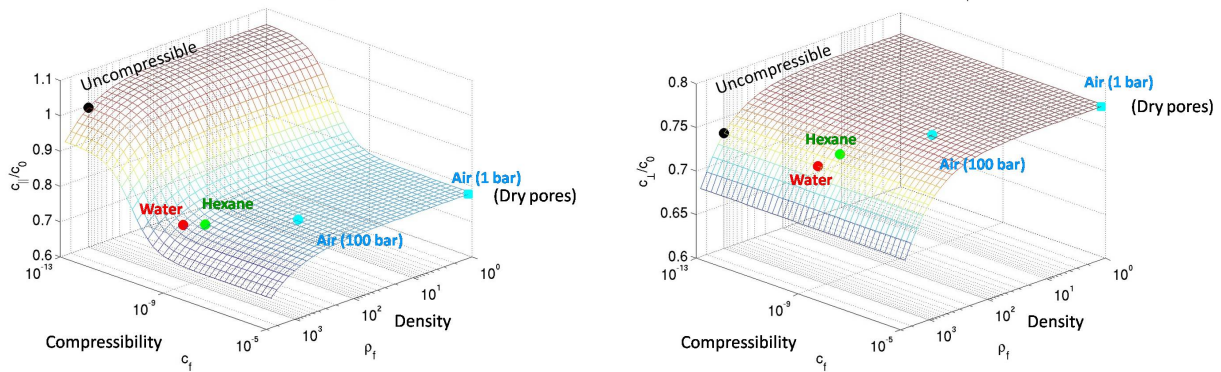

FIG. 3 – Compression (left) and shear (right) wave velocities calculated for a sample of sandstone imaged by X-ray tomography, in the low and intermediate frequency range, as functions of the fluid density and compressibility. The velocities are normalized by the corresponding values in the solid material. The position of some usual fluids is marked. The black dot corresponds to water regarded as incompressible.

The results for the two real rock samples and for unimodal reconstructed media are compared in Figure 4.
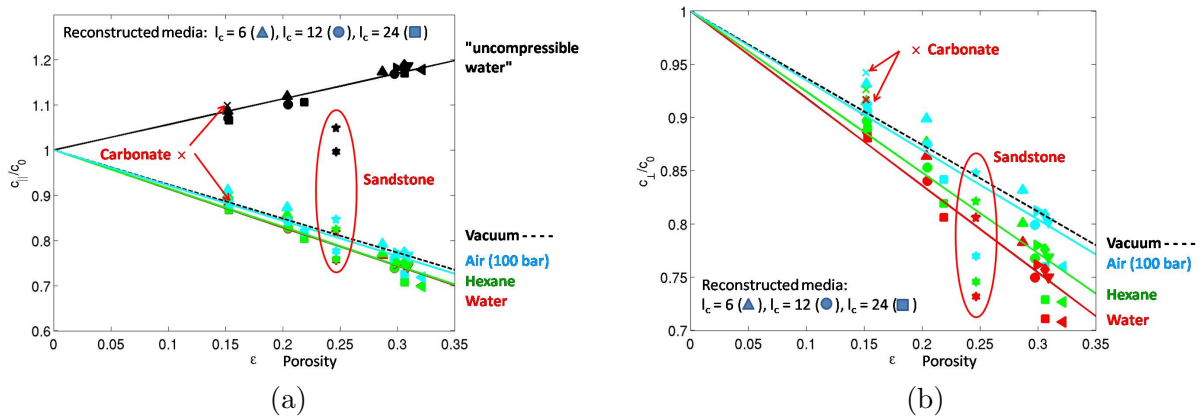

FIG. 4 – The fast compression (a) and shear (b) wave velocities as functions of the porosity for various interstitial fluids, in two real rock samples and in unimodal reconstructed media with various correlation lengths. The data for the real sandstone are for a subsampling of the tomographic image into 128^3 voxels of $5.6\mu m$ ($\star$) or into 64^3 voxels of $11.2\mu m$ ($*$). The straight lines are linear fits of the data for reconstructed media.

The agreement is good for $c_\parallel$, except for the sandstone saturated with water regarded as incompressible, but this is a rather unphysical case.

Although the hierarchy according to the kind of interstitial fluid is preserved, the agreement is quantitatively poorer for the shear wave velocity $c_\perp$. It is smaller (resp. larger) in the sandstone (resp. carbonated rock) than in a unimodal medium with the same porosity.

4 Conclusions

The global wave properties, namely velocity and attenuation coefficients, were derived by solving the Christoffel equation. Three types of waves were observed during propagation through the saturated media. The wave velocities were expressed explicitly which allows to analyze the effect of various parameters.

The theory has been applied to various kinds of porous media to study the influences of the mechanical properties of the interstitial fluid, the microstructures on the global characteristics of wave propagations. The numerical results are in good agreement with the analytical predictions.

Références

[1] Malinouskaya, I., Mourzenko, V.V., Bogdanov, I., Thovert, J.-F., Adler, P.M. 2007 JEMP, Grenoble.

[2] Malinouskaya, I., Mourzenko, V.V., Thovert, J.-F., Adler, P.M. 2008 Wave propagation through saturated porous media *Phys. Rev., E* **77**, 056307.

[3] Boutin, C., Auriault, J.L. 1990 Dynamic behaviour of porous media saturated by a viscoelastic fluid. Application to bituminous concretes. *Int. J. Engng. Sci.* **28**(11) 1157-1181.

[4] Biot, M.A. 1956 Theory of propagation of elastic waves in a fluid-saturated porous solid. I. Low-frequency range. II. Higher frequency range. *J. Acoust. Soc. Am* **28**(2) 168-191.